# The Identification of Ligand Features Essential for PXR Activation by Pharmacophore Modeling†

Daniela Schuster and Thierry Langer*

Department of Pharmaceutical Chemistry, Institute of Pharmacy, University of Innsbruck, Innrain 52, A-6020 Innsbruck, Austria

Received September 14, 2004

Drug metabolizing enzymes and transporters are often involved in clinically relevant drug-drug interactions. These functional proteins can be induced by a wide range of xenobiotics. The induction is mediated by a group of receptors known as orphan nuclear receptors. The pregnane X receptor (PXR) is a member of this receptor family and regulates the expression of multiple Cytochrome P450 enzyme families (e.g. CYP 3A and 2B), phase II enzymes (e.g. UDP glucuronosyl transferases), and transporters (e.g. multidrug resistance protein 1). The software package Catalyst was employed to derive pharmacophore models for PXR activation. A structure based pharmacophore hypothesis and several ligand based ones were compared in order to identify ligand receptor interactions essential for receptor activation. The results suggest that hydrogen bonding to Gln285 is indispensable for PXR activation. Most ligands were found to form a second hydrogen bond to His407. Hydrophobic interactions are not essential for receptor activation but contribute to ligand affinity. Highly active compounds share up to five hydrophobic features that allow the ligand to occupy large areas of the predominantly hydrophobic binding pocket.

## INTRODUCTION

In drug discovery and development not only pharmacological properties of potential new drugs come into account but also much attention lies on a compound's toxicology, ADME properties, and safety profile. Extensive preclinical studies address these qualities of a drug candidate before it can be administered to humans.[1] The earlier these aspects can be pre-estimated in the drug development process, the sooner promising drug candidates can be extracted from compounds most likely to become drugs.

In recent years, computational approaches have gained much importance in the early drug discovery process. Aside from e.g. receptor studies or lead discovery, molecular modeling can be employed for an appraisal of side effects and pharmacokinetic interactions of a drug candidate. Computational models for the prediction of these properties can be found in the literature in abundance.[2−5]

Drug metabolizing enzymes and transporters are often involved in clinically relevant drug-drug interactions. The transcription of many of these functional proteins involved in pharmacokinetics is regulated by a nuclear receptor called pregnane X receptor (PXR). For instance, the drug metabolizing enzymes belonging to the cytochrome P450 families CYP2B6, CYP3A4, CYP2C8, CYP2C9, the intestinal transporter MDR1, and human multidrug resistance proteins (MRP1 and MRP2) are regulated by PXR.[6] The transcriptional activation requires the binding of endogenous or exogenous ligands and recruitment of a coactivator, the formation of a heterodimer with the retinoid X receptor (RXR), and the binding of the heterodimer to the xenobiotic response element in the target gene promoter region.[7]

Although PXR is known as a very prominent xenobiotic receptor, it responds to a wide array of endogenous chemicals as well. By doing so, PXR has implications in several important physiological and pathological conditions:

Bile acids constitute a family of PXR ligands. Excess accumulation of bile acids has been shown to cause cholestasis (gall stones). PXR acts as a lithocholic acid (a bile acid) sensor and plays an essential role in detoxification of cholestatic bile acids. An activation of PXR by bile acids or other inducers causes the induction of CYP3A, an enzyme that facilitates the detoxification of bile acids.[8]

Bile acid intermediates formed during cholesterol catabolism also function as PXR agonists. PXR activation induces CYP3A mediated hydroxylation and clearance of potentially toxic bile acid intermediates. It seems that there exists a feed forward regulatory or salvage pathway, in which potentially toxic bile acid intermediates activate PXR and therefore induce their own metabolism and clearance to avoid accumulation and toxic effects.[8]

Besides its role in the detoxification of bile acids, PXR plays a pivotal role in bilirubin clearance and jaundice. Bilirubin, the catabolic byproduct of heme proteins, can accumulate in the blood and cause hepatotoxic and neurotoxic effects. UDP glucuronosyl transferase 1A1 (UGT1A1), a key enzyme for bilirubin clearance, is regulated by PXR. Other enzymes and transporters important for bilirubin clearance include the organic anion transporter polypeptide 2 (OATP2), glutathione S-transferases A1 (GSTA1), and GSTA2, all mediated by PXR. OATP2 reduces blood bilirubin levels by facilitating bilirubin uptake from blood into hepatocytes. GSTA1 and 2 reduce bilirubin back efflux

* Corresponding author phone: (+43) 512/507-5252; fax (+43) 512/507-5269; e-mail: Thierry.Langer@uibk.ac.at.

† Parts of this study were presented as a Poster at the EURO-QSAR 2004.

10.1021/ci049722q CCC: $30.25 
Published on Web 01/22/2005

from hepatocytes into blood.[7] If PXR constitutes a target to treat diseases as jaundice or bile acid induced hepatotoxicity remains to be determined.

The identification of a common pharmacophore for PXR ligands would be useful to predict potential drug-drug interactions or find lead compounds for an evaluation of PXR activators as new drugs.

## EARLIER APPROACHES

A ligand based PXR pharmacophore model has been described in the literature before;[9] however, the model was generated using the HypoGen algorithm of Catalyst[10] which is dedicated to estimate a compound's activity on a target, not to identify common features of active ligands.[11] The HypoGen model of Ekins et al. was compared with information retrieved from X-ray crystal structures of PXR. At that time, only crystal structures without a cocrystallized coactivator were available. In these crystal structures, a single ligand was observed in three different binding positions, so no defined binding mode could be observed.[12] In the meantime, a crystal structure of PXR cocrystallized with SR12813 and a coactivator peptide was published. This structure − referred to as 1NRL in the PDB − revealed a stabilized binding pocket in which the ligand binds in a single conformation.[13] In this crystal structure, PXR was crystallized as a homodimer at a resolution of 2.0 Å.

We are confident that this structure provides more accurate and new information on the PXR ligand binding domain. The examination of this new crystal structure together with a ligand based common feature pharmacophore model can help to understand PXR activation by structurally diverse ligands.

## MATERIALS AND METHODS

The computational molecular modeling studies were carried out using a Silicon Graphics Octane R12000 workstation running IRIX 6.5.10.

Two complementary approaches were used to identify essential patterns of PXR activation. First, a structure based approach was performed. Binding information derived from the X-ray crystal structure 1NRL was converted into a manually constructed pharmacophore model in the Catalyst software package version 4.9.[10] The PXR binding pocket was a further clue in recognizing inaccessible areas for putative ligands, and therefore information on the size of the binding site was included into the model by a set of defined excluded volume spheres. The evaluation of a test set provided information if this pharmacophore model described compound properties shared by structurally diverse PXR activators. The structure based model was then extended with ligand features not directly interacting with the ligand binding domain to determine whether other highly active PXR activators fit into the same pharmacophore.

Second, a ligand based approach was used to identify common features of structurally diverse receptor activators. The compounds of the training and test set were extracted from the SciFinder database,[14] imported into Catalyst, and submitted to energy minimization and conformational analysis (max. number of conformers = 250, generation type: best quality, energy range = 20 kcal/mol of minimum).[11] Using the HipHop algorithm of Catalyst,[11] a pharmacophore model for highly active compounds and general models for PXR ligands were built. For each training set, 10 hypotheses were returned by the hypotheses generation process. The pharmacophore features considered for the models were hydrogen bond acceptors (HBA) and hydrophobic features. These features were chosen after a careful analysis of chemical features present in known PXR ligands. After assessing all 10 hypotheses, a search in our in-house database of known PXR ligands was performed in Best Flexible Search mode to determine which hypothesis identified the most PXR ligands correctly as active.

By using the Shape algorithm of Catalyst,[11] spatial information of highly active compounds can be converted into a model. A shape excludes compounds that do not fit in the same space as the template molecule(s) and helps to reduce abundant hitlists derived from database mining.

A search in our in-house database (the so-called stockroom-database) of known PXR ligands was conducted with all pharmacophore models. This database consists of 53 compounds with known PXR activation properties, 9 (17%) of them classified as highly active, 17 (32%) as mediocre active, and 27 (51%) as poorly active or completely inactive (Table 2). All training and test set compounds are derived from the stockroom database.

**Table 1.** 30 PXR Ligands and 2 Nonligands Used as a Test Set for Hypothesis A[c]

| compound name | PXR activity[a] | classification by Hypothesis A[b] |
|---|---|---|
| lovastatin | +++[15] | ++ |
| nifedipine | +++[16] | +++ |
| rifampicin | +++[17] | + |
| sr12813 | +++[17] | +++ |
| troglitazone | +++[18] | +++ |
| 5$\beta$-pregnane-3,20-dione | ++[17] | + |
| clotrimazole | ++[17] | ++ |
| corticosterone | ++[18] | + |
| cortisol | ++[16] | + |
| estradiol | ++[18] | + |
| lithocholic acid | ++[19] | ++ |
| metyrapone | ++[20] | ++ |
| spironolactone | ++[18] | - |
| tcpobop | ++[17] | +++ |
| targretin | ++[18] | + |
| aldosterone | +[16] | - |
| 17$\alpha$-hydroxyprogesterone | +[18] | + |
| 3-keto lithocholic acid | +[19] | + |
| cholesterol | +[16] | + |
| dexamethasone | +[17] | ++ |
| dihydrotestosterone | +[18] | ++ |
| hypericin | +[21] | + |
| kaempferol | +[21] | - |
| myricetin | +[21] | - |
| PCN | +[17] | + |
| phenobarbital | +[18] | - |
| pregnenolone | +[18] | + |
| quercetin | +[21] | - |
| rutin | +[21] | - |
| scopoletin | +[21] | - |
| cortisone | -[18] | ++ |
| docetaxel | -[22] | - |

[a] Reported activity: -: inactive; +: $EC_{50}$ > 10 $\mu$M or PXR activation 1−2-fold; ++: $EC_{50}$ > 1−10 $\mu$M or PXR activation 2−5-fold; +++: $EC_{50}$ < 1 $\mu$M or PXR activation > 5-fold. [b] Catalyst classification by BestFit: -: not recognized by Hypothesis A; +: BestFit value 0−1.49; ++: BestFit value 1.5−2.99; +++: BestFit value 3−4. [c] 73% of active compounds were identified correctly; however, one inactive substance was assessed active.

**Table 2.** Validation of the Five PXR Activation Hypotheses by Assessing All 54 Stockroom Database Compounds in Categories of Activity

| | | classification by | | | | |
|---|---|---|---|---|---|---|
| compound | in vitro PXR activity[a] | Hypothesis A[b] | Hypothesis B[c] | PXR-HipHopA[d] | PXRHip-HopC.06[e] | PXRHip-HopD.07[f] |
| clotrimazole | +++ | ++ | - | - | ++ | - |
| dexamethasone-*tert*-butylacetate | +++[15] | ++ | - | - | +++ | +++ |
| hyperforin | +++[21] | +++ | + | +++ | +++ | +++ |
| lovastatin | +++ | ++ | - | - | +++ | +++ |
| nifedipine | +++ | +++ | - | - | +++ | +++ |
| paclitaxel | +++[22] | - | - | + | +++ | +++ |
| rifampicin | +++ | + | + | ++ | +++ | +++ |
| SR12813 | +++ | +++ | + | +++ | +++ | ++ |
| troglitazone | +++ | ++ | - | - | +++ | +++ |
| 5α-pregnane-3,20-dione | ++[16] | ++ | - | - | ++ | ++ |
| 5α-pregnane-3α-ol-11,20-dione | ++[16] | + | - | - | ++ | +++ |
| 5α-pregnane-3α-ol-20-one | ++[16] | ++ | - | - | ++ | ++ |
| 5β-pregnane-3,20-dione | ++[16] | + | - | - | ++ | +++ |
| 5β-pregnane-3α,20β-diole | ++ | + | - | - | ++ | ++ |
| corticosterone | ++ | + | - | - | ++ | +++ |
| cortisol | ++ | + | - | - | ++ | +++ |
| estradiol | ++ | + | - | - | + | ++ |
| lithocholic acid | ++ | ++ | - | - | +++ | +++ |
| metyrapone | ++ | ++ | - | - | + | ++ |
| mifepristone | ++[17] | ++ | - | - | +++ | ++ |
| phenobarbital | ++ | - | - | - | - | ++ |
| progesterone | ++[16] | + | - | - | ++ | ++ |
| spironolactone | ++ | - | - | - | ++ | +++ |
| targretin | ++ | + | - | - | +++ | - |
| TCPOBOP | ++ | +++ | - | - | ++ | +++ |
| umbelliferone | ++[21] | - | - | - | - | - |
| 17α-hydroxypregnenolone | +[18] | + | - | - | ++ | ++ |
| 17α-hydroxyprogesterone | + | + | - | - | ++ | +++ |
| 3-keto lithocholic acid | + | + | - | - | +++ | +++ |
| aldosterone | + | - | - | - | + | +++ |
| amentoflavone | +[21] | ++ | - | - | +++ | +++ |
| beta-sitosterol | +[21] | + | - | - | +++ | - |
| cholesterol | + | + | - | - | +++ | - |
| cyproterone acetate | +[18] | ++ | - | - | +++ | +++ |
| dexamethasone | + | ++ | - | - | ++ | +++ |
| DHEA | +[18] | + | - | - | - | ++ |
| dihydrotestosterone | +[18] | ++ | - | - | + | ++ |
| hypericin | + | + | - | - | ++ | ++ |
| hyperoside | +[21] | - | - | - | - | +++ |
| isoquercitrin | +[21] | - | - | - | - | +++ |
| kaempferol | + | - | - | - | - | ++ |
| luteolin | +[21] | - | - | - | - | ++ |
| myricetin | + | - | - | - | - | - |
| PCN | + | + | - | - | ++ | ++ |
| pregnenolone | + | + | - | - | ++ | ++ |
| pseudohypericin | +[21] | + | - | - | +++ | +++ |
| quercetin | + | - | - | - | - | ++ |
| quercitrin | +[21] | - | - | - | - | +++ |
| rutin | + | - | - | - | - | +++ |
| scopoletin | + | - | - | - | - | ++ |
| cortisone | - | ++ | - | - | ++ | +++ |
| docetaxel | - | - | - | - | +++ | +++ |
| LG268 | -[22] | ++ | - | - | +++ | ++ |

[a] Reported in vitro activity: -: inactive; +: $EC_{50}$ > 10 μM or PXR activation 1−2-fold; ++: $EC_{50}$ > 1−10 μM or PXR activation 2−5-fold; +++: $EC_{50}$ < 1 μM or PXR activation > 5-fold. [b] Catalyst classification by BestFit: -: not recognized by Hypothesis A; +: BestFit value 0−1.49; ++: BestFit value 1.5−2.99; +++: BestFit value 3.00−4.00. [c] As no fit value computation from "OR" combined hypotheses is possible, there is only a distinction of "identified as active" (+) or "not identified as highly active" (−). [d] Catalyst classification by BestFit: -: not recognized by PXR−HipHopA; +: BestFit value 0−1.49; ++: BestFit value 1.5−2.99; +++: BestFit value 3.00−7.00. [e] Catalyst classification by BestFit: -: not recognized by PXR−HipHopC.06; +: BestFit value 0−1.49; ++: BestFit value 1.5−2.99; +++: BestFit value 3.00−4.00. [f] Catalyst classification by BestFit: -: not recognized by PXR−HipHopC.06; +: BestFit value 0−0.49; ++: BestFit value 0.50−2.49; +++: BestFit value 2.50−3.00.

An overlay of the HipHop pharmacophore model with the crystal structure derived model was conducted by using the Compare algorithm of Catalyst.[11]

## RESULTS AND DISCUSSION

**Structure Based Approach.** The crystal structure 1NRL consists of a PXR homodimer cocrystallized with the coactivator peptide SRC-1 and the ligand SR12813 in each monomer. In both ligand binding domains, SR12813 (Figure 3) is bound in a single orientation. When comparing the contact sites between the ligand and the receptor protein, an equal binding mode could be observed. However, additional contacts between the coactivator peptide and PXR could be found in the monomer chain B.[13] Therefore, the B chain was

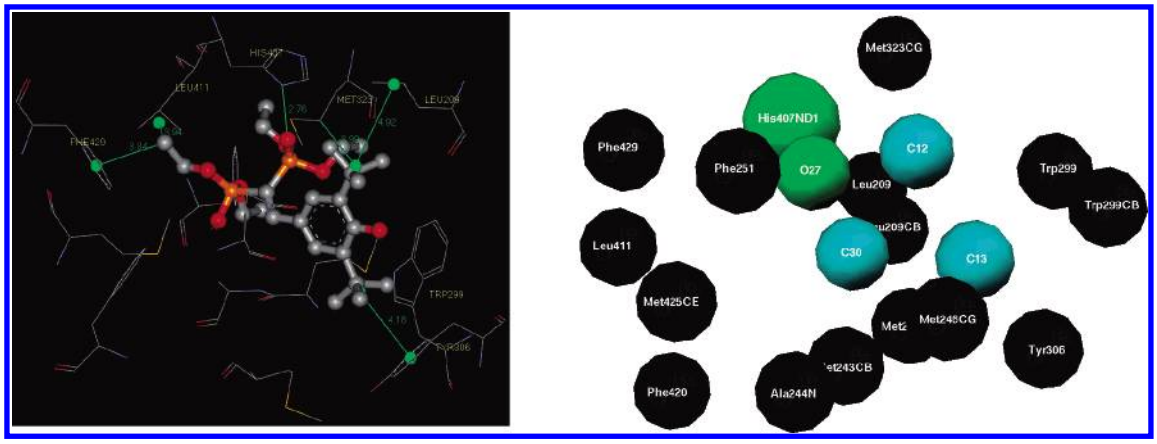


**Figure 1.** Left: the binding pocket of 1NRL, chain B. The ligand SR12813 is shown in ball-and-stick style, distances [Å] of contact points between SR12813 and PXR are monitored in green. Right: Hypothesis A. The HBA is shown in green, hydrophobic features in turquoise, and excluded volume spheres in black. The features are named after the corresponding atoms or structures in 1NRL.

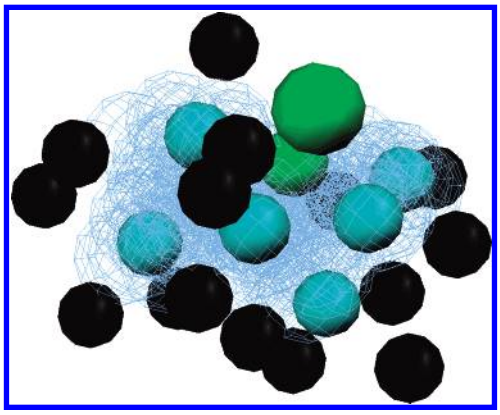

**Figure 2.** Hypothesis B consisting of one HBA (green), six hydrophobic features (turquoise) − three of them defined as "leave one out" -, 15 excluded volume spheres (black), and a combined shape of SR12813 and rifampicin (blue).

chosen for further investigation. After the extraction of the binding pocket from the rest of the protein the sites of interaction were examined. SR12813 accepts a hydrogen bond from His407. Hydrophobic interactions contribute to ligand binding at Phe429, Leu411, Met323, Leu209, and Tyr306. The aromatic ring of the ligand is not in direct contact with the binding pocket. Three ethyl residues extend into a large hydrophobic pocket. Ala244, Met243, Met246, Phe251, Trp299, Phe420, and Met425 flank the binding pocket without directly interacting with any structural feature of SR12813. The transformation of the binding information patterns of 1NRL into a Catalyst pharmacophore model resulted in Hypothesis A consisting of one HBA, three hydrophobic features, and 15 excluded volume spheres ($r$=1.5 Å) representing the amino acid residues that define the binding pocket (Figure 1).

To evaluate the ability of Hypothesis A to identify a wide range of PXR activators, a test set consisting of 30 PXR ligands and two nonligands was submitted to classification by the model. 22 compounds were correctly identified as active. However, one out of two inactive compounds was also assigned active by Hypothesis A (Table 1).

The five highly active compounds included in the test set were classified well (+++ or ++) except for rifampicin which was estimated poorly active (+). Most of the 10 compounds reported as moderately active PXR ligands were assessed correctly (++, three compounds) or too weak (+, five compounds). Spironolactone was classified as inactive (−), while TCPOBOPs activity was overestimated (+++). Most of the 15 weakly active compounds were estimated as inactive (-, seven compounds) or poorly active (+, six compounds). Dexamethasone and dihydrotestosterone were classified as too active (++). Interestingly, five of the seven weak PXR activators assessed inactive are phytogenic compounds. This aspect is attended to in the ligand based pharmacophore modeling section.

As nonligands such as cortisone can show the same chemical features and similar spatial properties as PXR ligands, e.g. cortisol, Hypothesis A is not able to distinguish these much related structures, so false positive results will be found in the database search hitlist. Fitting into Hypothesis A can therefore only constitute a first indicator for compound activity on PXR.

The evaluation of PXR ligands as therapeutic targets − e.g. in cholestasis − requires the identification of selective and potent agonists. Hypothesis A is far too general to serve as a tool for lead identification as described above. A more selective hypothesis which was able to recognize potent PXR ligands without providing many false positive hits from a database search had to be generated.

As SR12813 is a potent ligand of PXR, it was assumed that not only direct interaction sites between the receptor and the ligand but also other chemical features of SR12813 play a role in receptor affinity as well. Three hydrophobic features (from three ethyl groups) were added to the model resulting in a hypothesis consisting of one HBA, six hydrophobic features, and 15 excluded volume spheres. This more sophisticated hypothesis could only identify SR12813 as an active compound in the stockroom database. Other potent PXR ligands such as hyperforin or rifampicin only mapped five of the six hydrophobic spheres contained in the new hypothesis. After a careful analysis of active ligand feature mapping, three of the hydrophobic features − C12, C23, and C30 − were defined as "leave one out" features which means that one of these features may be ignored when fitting a compound into the model. To restrict the hitlist only to compounds with similar spatial dimensions as other potent PXR ligands, the new hypothesis ("Hypo1NRL-B") was extended by a combined shape. The two highly active ligands SR12813 and rifampicin were fitted into the model, trans-

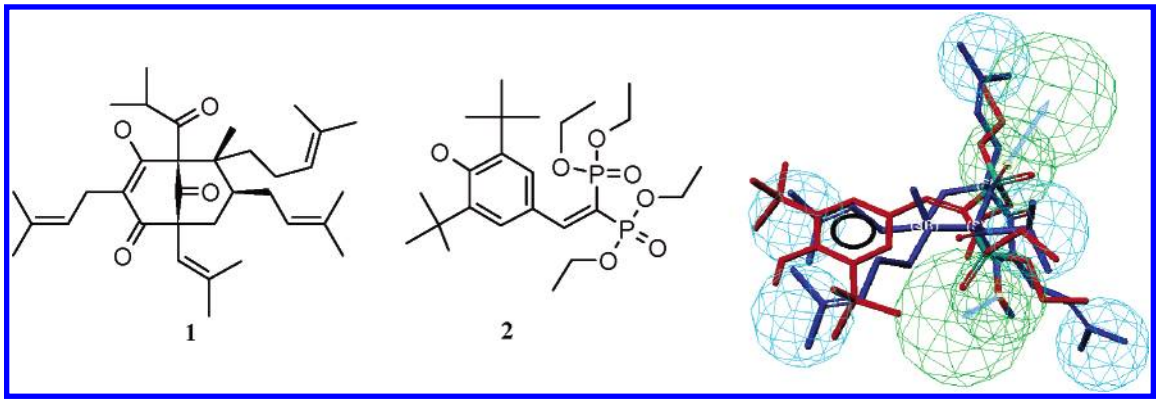


**Figure 3.** The compounds SR12813 (**1**) and hyperforin (**2**) were used as training set for the hypothesis PXRHipHopA, a pharmacophore model for highly active PXR ligands. **1** (red) and **2** (blue) are shown superimposed onto the hypothesis PXRHipHopA consisting of two HBA and five hydrophobic features.

ferred into shape queries, and combined by the Boolean operator "OR". Recapitulating, the hypothesis for potent PXR activators − "Hypothesis B" − consists of one HBA, six hydrophobic features of which three are defined as "leave one out", 15 excluded volume spheres, and a combined shape of SR12813 and rifampicin (Figure 2).

When performing a search in our in-house database of known PXR ligands, Hypo1NRL-B assessed SR12813, hyperforin, rifampicin, TCPOBOP, and nifedipine as active. Hypothesis B was able to identify the compounds SR12813, hyperforin, and rifampicin, as active, all of which are known as potent or moderate PXR ligands (Table 1). No weakly active or nonligand compounds mapped Hypo1NRL-B or Hypothesis B. As an additional test, we used our in-house database of commercial drugs (2361 compounds, all currently marketed drugs in Austria) where it can be assumed that PXR binding would cause noticeable side effects that would be known. When screening this database with Hypothesis B, we obtained a hit rate of 1.6% indicating that the rate of false positive ones is in a very low range. It can therefore be assumed that compounds returning as hits from a database search with these hypotheses are promising candidates for biological testing on PXR activity.

**Ligand Based Pharmacophore Model for PXR Ligands.** The structure based pharmacophore for PXR ligands reveals multiple sites of possible interactions; however, some highly active compounds only occupy a part of all possible interaction sites and leave others out. Accordingly, not all interaction sites in the PXR binding pocket seem to be equally important for PXR activation. Furthermore, only the binding properties of one single ligand (SR12813) could be explored because all other PXR crystal structures lack a cocrystallized coactivator molecule and are therefore not suitable for a direct comparison. To explain crucial ligand features for PXR activation, more information on the ligand properties had to be gained.

A ligand based approach allows an identification of chemical features common to all agonists/antagonists of a receptor assumed that they all have the same binding mode. A pharmacophore model for human PXR receptor ligands was reported in the literature before;[9] however, this model was generated using the HypoGen algorithm of Catalyst. HypoGen generates hypotheses which features contain a certain tolerance and weight that fit to the features of the training set and that correlate to the activity data. Generally, a training set for a HypoGen hypothesis should contain more than 16 structurally diverse compounds with a wide range of activity data (4−5 orders of magnitude).[23] The training set of the reported PXR HypoGen hypothesis consisted of only 12 compounds with an $EC_{50}$ from 0.023 (hyperforin) to ">10" (e.g. dexamethasone). The model consisted of one HBA and four hydrophobic features, similar to our structure based pharmacophore. The derived hypothesis was compared to crystal structures of PXR cocrystallized with SR12813; however, at that time no crystal structure with a cocrystallized coactivator was available. The later published PXR crystal structure in complex with a coactivator peptide and the ligand SR12813 (1NRL in the PDB) revealed a stabilized binding pocket and modified interaction sites compared to the previously obtained data.

To obtain accurate information on common features of PXR activators, three pharmacophore models were generated using the HipHop algorithm of Catalyst. HipHop generates common feature pharmacophore models from a set of compounds known to be active on a certain target molecule. The features consist of generalized chemical functions that simulate those characteristics necessary for receptor binding.[24] One of our models is based only on highly active compounds; the others are derived from a broader basis of PXR ligands.

*Pharmacophore Model for Two Highly Active PXR Activators.* A HipHop pharmacophore model based on two highly active PXR activators − SR12813 and hyperforin − revealed similar, although not the same, features as the structure based model (Figure 3).

As indicated by the structure based model, highly active PXR ligands share a predominantly hydrophobic character (five hydrophobic features). The role of HBAs is underscored by the ligand based model; it contains even two HBA features. An examination of the binding pocket of 1NRL suggests Gln285 as the corresponding amino acid residue to a second HBA of the ligand. In 1NRL, Gln285 forms no direct H-bond with the ligand SR12813; however, it interacts with a water molecule that is nearly in the range for forming a hydrogen bond with atom O20 of the ligand (Figure 4). In X-ray crystallography, waters are fit to "left over" density, so their positions are typically inaccurate. It is therefore justifiable to assess this water molecule as hydrogen bonding partner for the ligands.

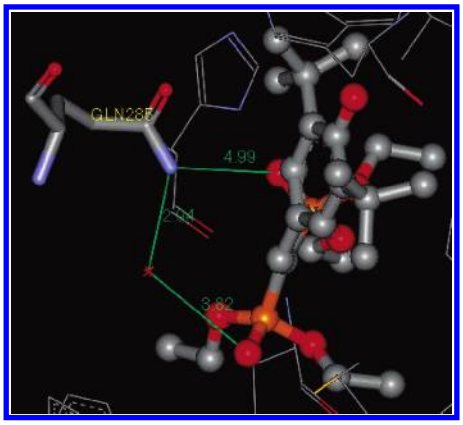


**Figure 4.** Gln285 shows no direct interaction with the ligand in 1NRL; however, a hydrogen bond via a water molecule could easily be formed.

If other ligands such as hyperforin form hydrogen bonds to Gln285 via this water molecule or directly remains open until further crystallographic research.

A search in our in-house database of known PXR ligands with PXRHipHopA returned two of the remaining four highly active PXR ligands as hits: rifampicin and paclitaxel. The other two potent PXR activators − troglitazone and nifedipine − were not able to map all features of PXRHipHopA. It should be underscored that a very similar compound to paclitaxel − docetaxel, inactive on PXR − was not included in the hitlist.

A search in our in-house database of commercial drugs returned a hit rate of 1.9%. Again, a very low range of false positive hits can be expected for database mining experiments with PXRHipHopA.

*Common Feature Model for PXR Ligands.* After the identification of common features for highly active PXR ligands, a more general pharmacophore model was created to investigate, which of these features are shared by most PXR activators. A training set of 15 known active compounds (Figure 5) including **1** and **2** was submitted to the hypotheses generation process using the HipHop algorithm of Catalyst.

Each of the hypotheses from this series was not able to distinguish the two inactive compounds implemented in the stockroom database from the active ones. The hypothesis PXRHipHopC.01 identified cortisone as inactive; however, it failed to assess cortisol active. All other hypotheses included both inactive compounds in the stockroom database search hitlist. The hypothesis that identified most of the stockroom compounds as active PXR ligands was chosen from the 10 retrieved hypotheses. Out of 36 active compounds, 30 (83%) were correctly identified by PXR-

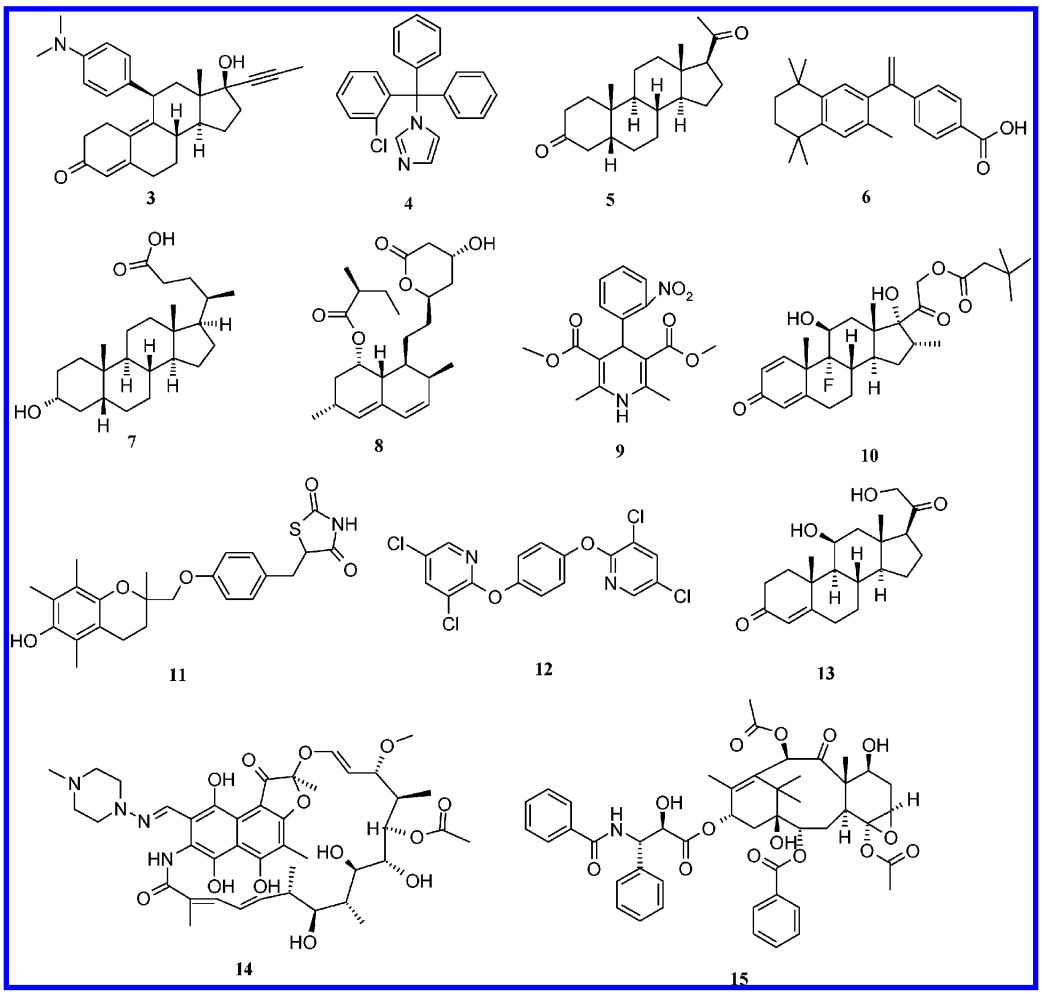


**Figure 5.** Compounds of the training set for a general PXR activation hypothesis (PXRHipHopC): mifepristone (**3**), clotrimazole (**4**), 5-$\beta$-pregnane-3,20-dione (**5**), targretin (**6**), lithocholic acid (**7**), lovastatin (**8**), nifedipine (**9**), dexamethasone *tert*-butyl acetate (**10**), troglitazone (**11**), TCPOBOP (**12**), corticosterone (**13**), rifampicin (**14**), and paclitaxel (**15**).

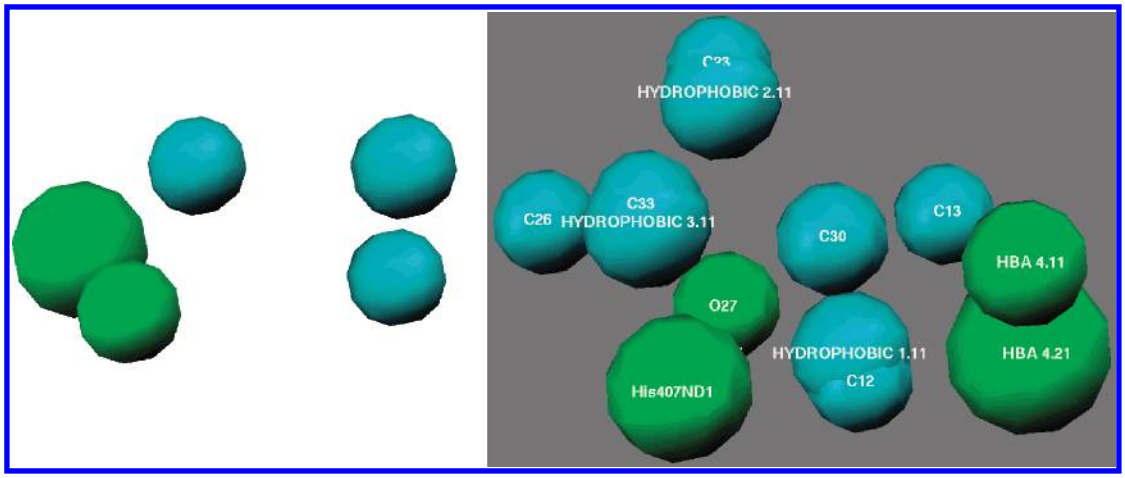


**Figure 6.** The hypothesis PXRHipHopC.06 shows features common to a major part of PXR ligands included in the stockroom database: one HBA and three hydrophobic features. The superimposition of the hypothesis PXRHipHopC.06 and Hypo1NRL-B reveals that three hydrophobic features each map each other well, while the HBAs are not located in the same region.

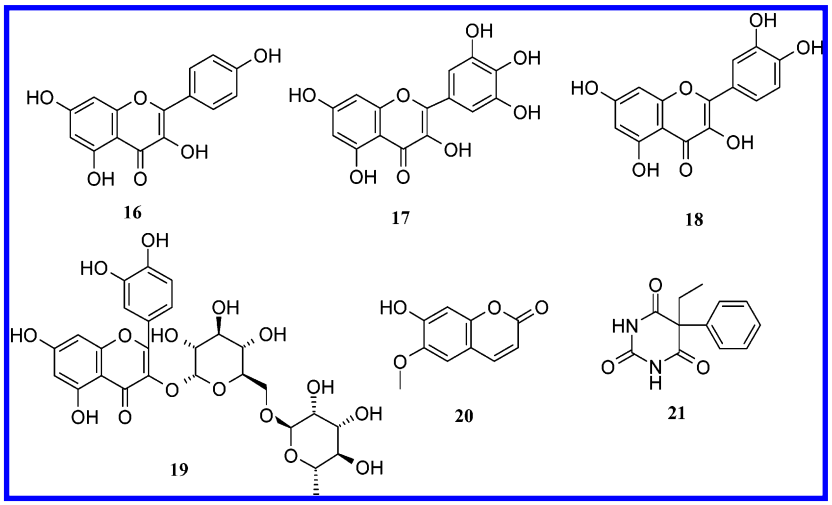


**Figure 7.** PXR activators that were identified as inactive by PXRHipHopC.06: kaempferol (**16**), myricetin (**17**), quercetin (**18**), rutin (**19**), scopoletin (**20**), and phenobarbital (**21**).

HipHopC.06 that consists of three hydrophobic features and one HBA (Figure 6).

Again, hydrophobic features constitute a major part of the pharmacophore model. Interestingly, only one HBA is included in this model. To determine if this HBA describes the hydrogen bond of SR12813 to His407 in 1NRL, PXRHipHopC.06 was compared with the hypothesis directly derived from the crystal structure (Hypo1NRL-B) by using the Compare algorithm of Catalyst. The fitting revealed that the three hydrophobic domains of the ligand based model match the hydrophobic regions around C12, C23, and C33 of SR12813 well while the HBAs are not located near each other (Figure 9). Therefore, it can be assumed that hydrogen bonding with His407 is beneficial for a ligands potency; however, it is not essential for PXR activation. The interaction with Gln285 via a hydrogen bond − even though this information cannot be derived directly from the crystal structure − seems to play a major role in receptor activation.

PXRHipHopC.06 succeeds in describing common features of a large number of structural diverse PXR activators. However, six active PXR ligands were classified as inactive by the model (Figure 7).

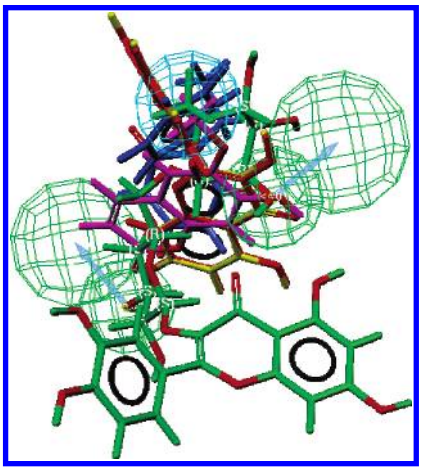

**Figure 8.** Compounds of the training set fitted into PXRHipHopD.07 consisting of two HBAs and one hydrophobic feature.

When comparing these results with the test set validation of Hypothesis A, it attracted our attention that all these compounds were misclassified by both hypotheses suggesting a different binding mode. It should be mentioned that all misclassified compounds constitute weak PXR activators compared with hyperforin, SR12813, or rifampicin. A chemical features analysis of the misclassified structures

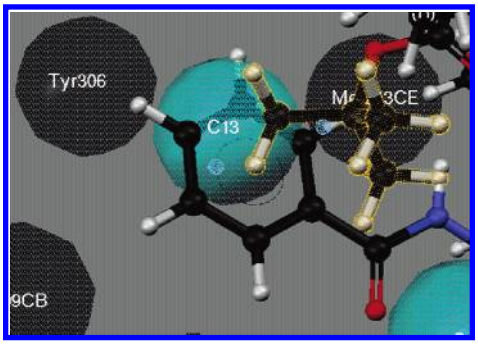


**Figure 9.** The phenyl residue of paclitaxel interacts with Tyr306 by a $\pi-\pi$ interaction. The *tert*-butyl group of docetaxel (highlighted) is not able to equally interact with Tyr306, so docetaxel is not able to activate PXR.

revealed an abundance of HBAs (from three in phenobarbital up to eight in myricetin) and a shortage of hydrophobic regions (from none in myricetin up to two, e.g. in rutin). A HipHop pharmacophore model derived from all six misclassified compounds (Figure 8) resulted in a hypothesis consisting of two HBAs. When excluding myricetin from the training set, an additional hydrophobic feature was added to the hypothesis (PXRHipHopD). From 10 hypotheses derived from the hypotheses generation process, PXRHipHopD.07 (Figure 8) identified most known PXR ligands as active. From 36 PXR activators included in the stockroom database, 32 (89%) were identified correctly. Four PXR activators did not map all features: myricetin lacks a hydrophobic feature, cholesterol and clotrimazole only show one HBA, and targretin − even though it has two HBAs − only maps one of them when fitted into PXRHipHopD.07.

From these results it can be concluded that PXRHipHopD.07 describes not a different but a more general binding mode than PXRHipHopC.06.

Table 2 summarizes the hypotheses validation by classification of all compounds included in our stockroom database.

**Explanation of Different Binding Modes of Very Similar Molecules on PXR.** *Docetaxel/Paclitaxel.* By fitting into Hypo1NRL-B the different interaction of paclitaxel and docetaxel on PXR can be hypothesized. The only difference between the two structures lies in an phenyl residue of paclitaxel that is replaced by a *tert*-butyl group in docetaxel. The respective substructures interact with Tyr306 of the receptor protein (Figure 9).

Obviously, a $\pi-\pi$ stacking interaction is highly favored at this position, so paclitaxel can activate PXR easily. The *tert*-butyl group of docetaxel could not occupy this interaction site in any conformation.

*Cortisol/Cortisone.* While cortisol activates PXR, the presence of cortisone has no influence on PXR activity. The two compounds solely differ by an oxo/hydroxyl group at position 11, both chemical features which can act as HBAs. Therefore the different affinity to PXR cannot be explained by the presence or absence of certain functional groups. To ensure that the HBA feature at position 11 is involved in the interaction with the binding pocket, cortisol was fitted into the hypothesis PXRHipHopD.07, where the hydroxyl group at the respective position mapped well into a HBA feature. When performing the same experiment with cortisol, the oxo group at position 11 did not map a HBA feature (Figure 10).

As this theoretical approach suggests, the conformation of the molecule changes slightly but enough to prevent cortisone from activating PXR.

## CONCLUSION

It can be summarized that the only feature shared by all PXR ligands is one HBA. According to our studies, this might not be an H-bond to His407 but to Gln285 directly or via a water molecule. Most but not all PXR ligands possess a second hydrogen bond (to His407) and a hydrophobic feature. The hydrophobic interaction with Tyr306 might play a major role in PXR activation as suggested by the different activities of paclitaxel and docetaxel on the receptor. Additional hydrophobic interactions are not essential for PXR activation but seem to be beneficial for a ligands potency. As hypothesis PXRHipHopA.04 shows, highly active PXR ligands share up to seven common features of which five constitute hydrophobic regions. These chemical properties allow compounds to occupy large areas of the predominantly hydrophobic binding pocket and perform strong receptor activation.

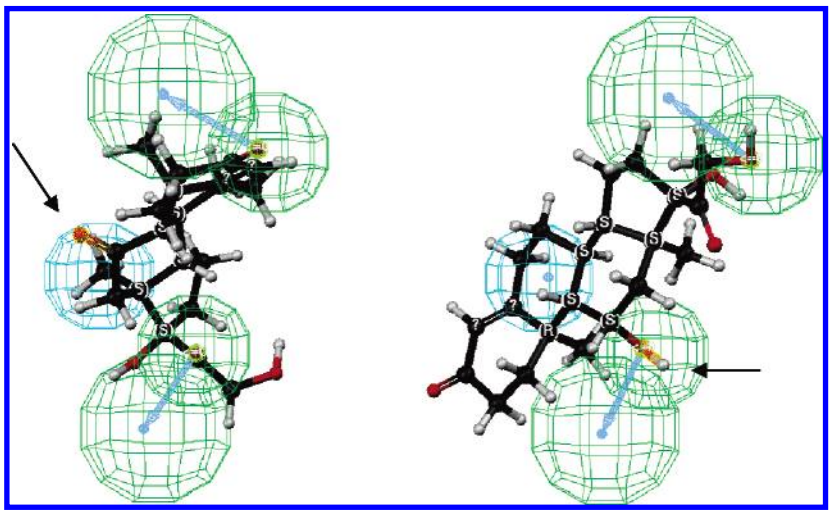

**Figure 10.** Cortisone (left) and cortisol (right) fitted into PXRHipHopD.07. The position 11 of the molecule is indicated by an arrow each. The inactive PXR ligand cortisone maps no HBA feature of the model; the 11-OH-group of cortisol fits well into one HBA sphere.

## ACKNOWLEDGMENT

We thank Dr. Eva Krovat for thoughtful reading of the manuscript.

## REFERENCES AND NOTES

(1) Pritchard, J. F.; Jurima-Romet, M.; Reimer Mark, L. J.; Mortimer, E.; Rolfe, B. et al. Making better drugs: Decision gates in nonclinical drug development. *Nat. Rev. Drug Discov.* **2003**, *2*, 542−553.

(2) Ekins, S.; Crumb, W. J.; Sarazan, R. D.; Wikel, J. H.; Wrighton, S. A. Three-dimensional quantitative structure−activity relationship for inhibition of human ether-a-go-go-related gene potassium channel. *J. Pharmacol. Exp. Ther.* **2002**, *301*, 427−434.

(3) Ekins, S.; Berbaum, J.; Harrison, R. K. Generation and validation of rapid computational filters for CYP2D6 and CYP3A4. *Drug Metab. Dispos.* **2003**, *31*, 1077−1080.

(4) Rao, S.; Aoyama, R.; Schrag, M.; Trager, W. F.; Rettie, A. et al. A Refined 3-dimensional QSAR of cytochrome P450 2C9: computational predictions of drug interactions. *J. Med. Chem.* **2000**, *43*, 2789−2796.

(5) Hou, T. J.; Xu, X. J. ADME Evaluation in Drug Discovery. 3. Modeling Blood-Brain Barrier Partitioning Using Simple Molecular Descriptors [Erratum for [*J. Chem. Inf. Comput. Sci*. 43, 2137−2152 2003]]. *J. Chem. Inf. Comput. Sci.* **2004**, *44*, 766−770.

(6) Ekins, S.; Mirny, L.; Schuetz, E. G. A Ligand-Based Approach to Understanding Selectivity of Nuclear Hormone Receptors PXR, CAR, FXR, LXRa, and LXRb. *Pharm. Res.* **2002**, *19*, 1788−1800.

(7) Xie, W.; Uppal, H.; Saini, S. P. S.; Mu, Y.; Little, J. M. et al. Orphan nuclear receptor-mediated xenobiotic regulation in drug metabolism. *Drug Discov. Today* **2004**, *9*, 442−449.

(8) Xie, W.; Radominska-Pandya, A.; Shi, Y.; Simon, C. M.; Nelson, M. C. et al. An essential role for nuclear receptors SXR/PXR in detoxification of cholestatic bile acids. *Proc. Natl. Acad. Sci. U.S.A.* **2001**, *98*, 3375−3380.

(9) Ekins, S.; Erickson, J. A. A pharmacophore for human pregnane X receptor ligands. *Drug Metab. Dispos.* **2002**, *30*, 96−99.

(10) Catalyst. *Catalyst software package*, *Vers. 4.9*; Accelrys Software Inc.: San Diego, CA.

(11) Catalyst. Catalyst software package, Tutorial Release 4.9. 2003.

(12) Watkins, R. E.; Wisely, G. B.; Moore, L. B.; Collins, J. L.; Lambert, M. H. et al. The human nuclear xenobiotic receptor PXR: Structural determinants of directed promiscuity. *Science* **2001**, *292*, 2329−2333.

(13) Watkins, R. E.; Davis-Searles, P. R.; Lambert, M. H.; Redinbo, M. R. Coactivator Binding Promotes the Specific Interaction Between Ligand and the Pregnane X Receptor. *J. Mol. Biol.* **2003**, *331*, 815−828.

(14) SciFinder Scholar 2003, http://www.cas.org./SCIFINDER/SCHOLAR/ Copyright by The American Chemical Society, Washington, DC.

(15) Lehmann, J. M.; McKee, D. D.; Watson, M. A.; Willson, T. M.; Moore, J. T. et al. The human orphan nuclear receptor PXR is activated by compounds that regulate CYP3A4 gene expression and cause drug interactions. *J. Clin. Invest.* **1998**, *102*, 1016−1023.

(16) Bertilsson, G.; Heidrich, J.; Svensson, K.; Asman, M.; Jendeberg, L. et al. Identification of a human nuclear receptor defines a new signaling pathway for CYP3A induction. *Proc. Natl. Acad. Sci. U.S.A.* **1998**, *95*, 12208−12213.

(17) Moore, L. B.; Parks, D. J.; Jones, S. A.; Bledsoe, R. K.; Consler, T. G. et al. Orphan nuclear receptors constitutive androstane receptor and pregnane X receptor share xenobiotic and steroid ligands. *J. Biol. Chem.* **2000**, *275*, 15122−15127.

(18) Jones, S. A.; Moore, L. B.; Shenk, J. L.; Wisely, G. B.; Hamilton, G. A. et al. The pregnane X receptor: A promiscuous xenobiotic receptor that has diverged during evolution. *Mol. Endocrinol.* **2000**, *14*, 27−39.

(19) Staudinger, J. L.; Goodwin, B.; Jones, S. A.; Hawkins-Brown, D.; MacKenzie, K. I. et al. The nuclear receptor PXR is a lithocholic acid sensor that protects against liver toxicity. *Proc. Natl. Acad. Sci. U.S.A.* **2001**, *98*, 3369−3374.

(20) Wright, M. C. The cytochrome P450 3A4 inducer metyrapone is an activator of the human pregnane X receptor. *Biochem. Soc. Trans.* **1999**, *27*, 387−391.

(21) Moore, L. B.; Goodwin, B.; Jones, S. A.; Wisely, G. B.; Serabjit-Singh, C. J. et al. St. John's wort induces hepatic drug metabolism through activation of the pregnane X receptor. *Proc. Natl. Acad. Sci. U.S.A.* **2000**, *97*, 7500−7502.

(22) Synold, T. W.; Dussault, I.; Forman, B. M. The orphan nuclear receptor SXR coordinately regulates drug metabolism and efflux. *Nat. Med.* **2001**, *7*, 584−590.

(23) Hong, L.; Sutter, J.; Hoffmann, R. HypoGen: An Automated System for Generating 3D Predictive Pharmacophore Models. *Pharmacophore Perception, Development, and Use in Drug Design*; International University Line: La Jolla, CA, 2000; pp 172−189.

(24) Clement, O. O.; Mehl, A. T. HipHop: Pharmacophores Based on Multiple Common-Feature Alignments. *Pharmacophore Perception, Development, and Use in Drug Design*; International University Line: La Jolla, CA, 2000; pp 70−84.

CI049722Q